RSC Advances

COMMUNICATION

View Article Online
View Journal | View Issue



Cite this: *RSC Adv.*, 2016, **6**, 22469

# Plant leaves as templates for soft lithography†

Wenming Wu,[ab] Rosanne M. Guijt,[c] Yuliya E. Silina,[d] Marcus Koch[d] and Andreas Manz*[ab]

Received 4th December 2015
Accepted 10th February 2016

DOI: 10.1039/c5ra25890a

www.rsc.org/advances



We report a simple fast, practical and effective method for the replication of the complex venation patterns of natural leaves into PDMS with accuracy down to a lateral size of 500 nm. Optimising the amount of crosslinker enabled the replication and sealing of the microvascular structures to yield enclosed microfluidic networks. The use of plant leaves as templates for soft lithography was demonstrated across over ten species and included reticulate, arcuate, pinnate, parallel and palmate venation patterns. SEM imaging revealed replication of the plants microscopic and sub-microscopic topography into the PDMS structures, making this method especially attractive for mimicking biological structures for *in vitro* assays. Flow analysis revealed that the autonomous liquid transport velocity in 1st-order microchannel was 1.5–2.2 times faster than that in the 2nd-order microchannels across three leaf types, with the sorptivity rule surprisingly preserved during self-powered flow through leaf-inspired vascularity from *Carpinus betulus*.

Biological microstructures have long been a source of inspiration for artists and scientists.[1] In engineering, biomimetic approaches have enabled the systematic study of nature-derived nano-, micro- and macroscopic structures. Perhaps most famous is the discovery of superhydrophobicity mimicking[2] the nano-microscopic surface morphology of the natural-leaf templates, such as *Strelitzia reginae*,[3,4] taro,[5] lotus and rice leaves.[6,7] Superhydrophobic surfaces have been utilized in a myriad of technological applications including anti-wetting[8,9] bubble bursting,[10] organic-proofing,[11] directional transportation,[12] antifogging,[13] superhydrophobicity–superhydrophilicity transition,[14,15] self-cleaning,[16–18] self-repairing interfaces.[19,20]

The diversity and organization of microvascular structures from plants has drawn significant attention, inspiring solutions in engineering modeling,[21] paleoecology hindcasting,[22] low-noise microelectronics,[23] thermal distribution,[24] the design of durable wind turbines,[25] green energy,[26] *etc.* Recent research revealed that both radius tapering and the ratio of daughter to parent branch areas in leaf veins are in strong agreement with Murray's law, and hence resemble the circulatory and respiratory systems.[27] In both cases, the sum of the cubes of each-order veins is conserved throughout the flow network.[28] This correlation provides great opportunities for leaf-inspired microfluidic devices in the creation of bio-realistic *in vitro* models. By selecting different venation types including reticulate, arcuate, parallel, pinnate and palmate, we foresee leaf-inspired microfluidic devices can be utilized for various applications, *e.g.*, cancer metastasis, microparticle separation, capillary electrophoresis and 3D microvessel engineering, *etc.*

Almost twenty years ago, microfluidic fabrication was revolutionised by the introduction of polydimethylsiloxane (PDMS) for casting from microstructured templates.[29] PDMS has become the most widely adopted material in fabricating microdevices[30–33] thanks to its ease of use, optical transparency and biocompatibility. The templates used for casting have ranged from structures made in multilayer tape,[34] SU-8 or other photoresists like Norland Optical Adhesive (NOA),[35] 3D printed resin,[36] printed circuit boards, or by simply gluing capillaries and other structures onto a substrate (*e.g.*, PMMA).[35,37]

Traditional fabrication techniques including inkjet printing, photolithography and chemical etching have all been used to produce "leaf inspired" microchannels.[38–40] Prof. A. Lewis' group printed a fugitive organic ink according to the microvasculature of ivy leaves.[36] After casting epoxy matrices, the ink could be removed at 80 °C under light vacuum, leaving a microvascular fluidic network. Other reports were based on traditional photolithography and soft lithography technologies to produce an SU-8 master for further replication into gel[38] or PDMS.[39] Photomasks were created by depositing chromium onto a leaf skeleton obtained by alkaline removal of the soft

[a]*Mechatronics Department, University of Saarland, Germany*
[b]*KIST Europe GmbH, 66123, Saarbrücken, Germany. E-mail: manz@kist-europe.de*
[c]*School of Medicine and ACROSS, University of Tasmania, Hobart, Australia*
[d]*INM-Leibniz Institute for New Materials, Campus D2 2, Saarbrücken, Germany*

† Electronic supplementary information (ESI) available. See DOI: 10.1039/c5ra25890a

tissue,[40] which was then used to transfer the microvascular network onto a silicon wafer.

Here we introduce a simpler alternative approach where microfluidic structures are directly replicated from plant leaves. In contrast with other microfabrication techniques, this highly economical approach only utilizes PDMS elastomer for microchip fabrication and eliminates the reliance for costly reagents, *e.g.*, fugitive ink,[36] photoresist,[38] developer[38–40] and corrosive chemicals.[39,40] Furthermore, clean room facilities and microfabrication equipment including inkjet printer,[36] mask aligners,[38–40] CNC milling,[47] or laser ablation are also waived here. Because a natural leaf template is directly utilized for microstructural definition, herein truly 3D (varied microchannel height all through the network) vascular structure is reproduced instead of 2D (same microchannel height all through the network) vascular structure as in previous reports.[36,38–40] Unlike other "leaf inspired" microfabrication techniques,[38–40] the surface topography of the leaves is also replicated, resulting in complex structured channel surfaces that may offer a much more realistic microenvironment for Lab-on-a-Chip based cell assays.[41–43] We anticipate this nature-inspired manufacturing methodology may open new opportunities by leading microfluidic based microvascular engineering towards more bio-realistic assays.

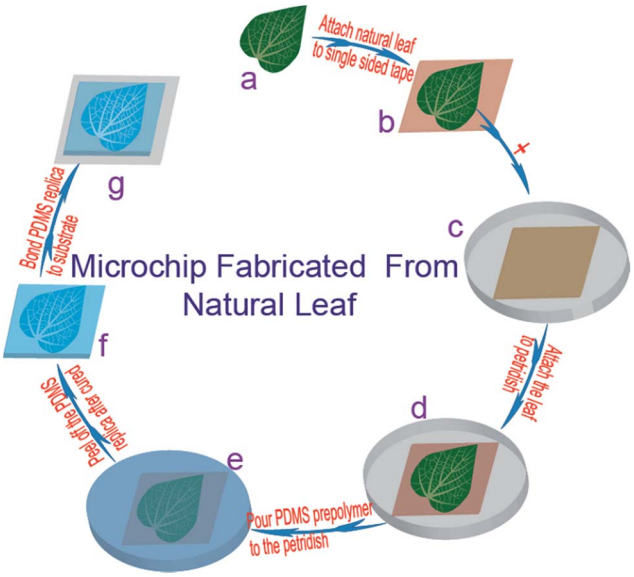


Fig. 1 Schematic steps of the direct replication of microvascular networks from natural leaves into a microfluidic PDMS device. The natural leaf (a) attached to single-sided tape (b) is mounted onto a Petridish (d) using double sided tape (c). The PDMS pre-polymer is poured over the leaf and cured (e) before the PDMS replica is removed (f). An enclosed microchannel is formed by sealing the PDMS replica with a glass or PDMS substrate after oxygen plasma treatment (g). The biomimetic chip is placed in an oven at 80 °C for 2 hours in order to stabilize bonding strength (g).

## Experimental

### Microchip fabrication

A schematic overview of the main steps in the use of plant leaves as templates for soft lithography is schematically depicted in Fig. 1. Leaves were removed from plants and rinsed under running water for one minute, and gently wiped using laboratory paper and blow dried using a $N_2$. On the same day, the leaf was attached to single-sided tape (Tesa 57176-00 Tesapack ultra-strong tr. 66 m: 50 mm wide) and then to a disposable Petri dish (Mit 3 Nocken Ø 90 mm, 391-0247) using double-sided tape (Tesa double side tape 10 m: 15 mm wide). PDMS (SYLGARD 184; Dow Corning, USA) was prepared by carefully mixing the PDMS prepolymer and cross linker in a 20 : 1 ratio, and degassed for 1 h in a vacuum desiccator to remove air bubbles. When pouring the PDMS into the Petri dish containing the leaf, any possible bubbles formed could automatically disappear after few minutes. The PDMS was cured in an oven (Binder, US PATS 4585923) at 45 °C for 24 h (Fig. 1f).

Next, the PDMS replica was cut using a box cutter and peeled off the template. The template was again covered with PDMS to protect it for further structure replication. An oxygen plasma system (Diener electronic: 0010915) was used to activate the surfaces of both PDMS replica and glass or PDMS substrates before bonding. Finally, the assembled devices were placed in the oven at 80 °C for two hours to increase bonding strength. Images of leaves templates were taken using a consumer CCD camera (Canon ED560D with macro-lens).

### Pressure-driven flow

A 5 mL disposable syringe was utilized to fill the microfluidic network. The syringe was filled with 2.5 mL of red ink (WATERMAN Fountain Pen Ink, Audacious Red S0110730) before the piston was withdrawn to the 4.3 mL mark. A 2 mm diameter inlet was punched in the PDMS replica of a leaf to connect with the central vein and connected with silicone tubing, sealed in place using uncured PDMS. A pipette tip (1–200 μL, UltraFine™, graduiert, VWR International GmbH) was used to connect the filled syringe with the microfluidic network. The system was pressurized by pushing the piston from the 4.3 mL mark to the 3.2 mL mark on the syringe, and fixed in this position using a metal wire (Fig. S6, ESI 1†).

### Scanning electron microscopy (SEM)

For correlative SEM analysis of the positive leaf and the negative PDMS replica, a FEI (Hilsboro, OR, USA) Quanta 400 FEG was used. Samples were investigated in low vacuum mode ($p$ = 100 Pa water vapor) at an accelerating voltage of 10 kV using the secondary electron (large field) detector (30 μm final lens aperture size; spot size 3; pixel dwell time 30 μs, image size 1024 × 884 pixels).

### Atomic force microscopy (AFM)

For AFM measurements 20 nm gold was sputtered on the PDMS replica to eliminate charging during investigation. A Nanowizard 3 (JPK Instruments, Berlin, Germany) operating in tapping mode was used to reveal the 3D structure of the replicated leaf surface. AFM tips from NANOSENSORS (Neuchatel, Switzerland), type PPP-NCLR were used for height measurements.

### Elastic modulus (*E*-modulus) of PDMS templates

Varying the degree of crosslinking in the polymer network allows tuning its mechanical properties in a wide range. To estimate mechanical properties of PDMS produced with different amount of crosslinking from the each of flat templates a cylinder with a 3 mm diameter was cut for the subsequent compression test performed under 25 °C with a TA DMA Q 800 instrument (TAINSTRUMENT, Eschborn, Germany).

### Head-space gas chromatography mass spectrometry

**(HS-GC-MS).** To verify the chemical stability of the produced PDMS templates HS-GC-MS analysis was performed. A gas sample of 500 μL at 50, 70 and 100 °C from the headspace above the sample (0.15 g) (5 min incubation time; agitator speed, 500 rpm; fill speed, 100 μL $s^{-1}$; injection speed, 500 μL $s^{-1}$) was injected by a PAL auto sampler (CTC Analytics, Zwingen, Switzerland) into the QP5050 (Shimadzu, Japan) GC-MS system. A Phenomenex (Torrance, CA, USA) ZB-WAX-plus column (30 m × 0.25 mm; film thickness 0.25 μm) was utilized for separation. An injection temperature of 200 °C (split ratio 1 : 35) was used, with the temperature program kept at 50 °C for 1 min, then raised to 200 °C at 20 K $min^{-1}$ and held at the final temperature 250 °C for 5 min. The column inlet pressure was adjusted to 100 kPa, giving a flow rate of 1.7 mL $min^{-1}$. The transfer line to the mass spectrometer and the source temperatures were 230 °C and 200 °C, respectively. Electron ionization (70 eV) mass spectra were recorded in the *m*/*z* range of 40–920.

## Results and discussion

### Leaf-inspired microfluidic devices

There is a large variation in the size, geometry and venation between leaves from different plant species, and in this work, leaves from *Tilia platyphyllos*, *Prunus cerasifera*, *Viburnum davidii*, *Prunus avium*, *Plantago lanceolate*, *Carpinus betulus*, *Fraxinus excelsior*, *Glechoma hederacea*, *Acer pseudoplatanus* and *Aegopodium podagraia* were all successfully replicated in PDMS.

Examples of leaves and their replicates of a reticulate, arcuate, parallel, pinnate and palmate venation are given in Fig. 2a–j, with close-up images of the microvascular channels in Fig. 2k–o. More information about microchip fabrication from other leaves is also added to Fig. S1 (ESI 1†). The widths of the first ordered channels were measured to be 0.54 mm, 0.81 mm, 1.20 mm, 0.82 mm and 0.43 mm for *Tilia platyphyllos*, *Aegopodium podagraia*, *Plantago lanceolate*, *Frangula alnus* and *Acer pseudoplatanus* leaves, respectively. Remarkably that, the 1st ordered channel in *Plantago lanceolate* was 2.8 times wider than in *Acer pseudoplatanus*. Across all species, the smallest veins were around 8 μm wide (Fig. S2, ESI 1†), much smaller than previous reports.[39,40] As the replicated vascular structures were copied from the outside of the leaf, internal structures like the phloem and xylem cannot be replicated by means of this method. The vascular geometry and size distribution across the bifurcating channels, however, was maintained as demonstrated by the reduction in channel width moving down from the first order or main vein as shown in Fig. 2k–o.

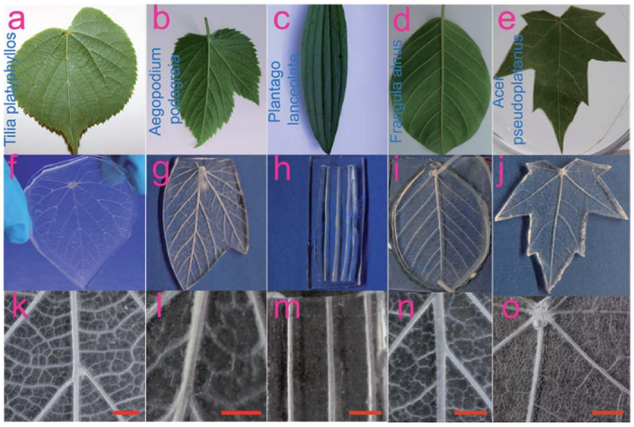


Fig. 2 Diversity in shape and venation in plant leaves. (a–e) Photographs of the fresh leaves; (f–j) photographs of PDMS replicates and (k–o) close-ups of the first order vein of *Tilia platyphyllos*, *Aegopodium podagraia*, *Plantago lanceolate*, *Frangula alnus* and *Acer pseudoplatanus*. Scale bar images (k–o) corresponds to 2.5 mm.

### Optimization of crosslinker : monomer ratio

Initially, the soft lithography experiment was carried out using the standard 1 : 10 crosslinker : monomer ratio, but the obtained structures could not be sealed in a leakage-tight manner to glass or PDMS substrates. This was hypothesized to be due to the stiffness of the PDMS preventing the textured leaf replica from sealing with the flat substrate. It is known that the stiffness of PDMS can be reduced when the amount of initiator reaches 1 : 20 ratio.[44,45] The soft lithography process was repeated using PDMS mixed in 1 : 15, 1 : 20 and 1 : 30 crosslinker : monomer ratios. The templates obtained using over 1 : 30 PDMS ratio were sticky to touch and left residues, indicating that PDMS was not be fully cured even when extending the curing time to days. For this reason PDMS template synthesized with 1 : 30 crosslinker : monomer ratio has been eliminated from the further experiments. The 1 : 20 ratio provided a PDMS template that was softer than the PDMS obtained using the 1 : 10 or 1 : 15 ratio (Table 1).

In addition, PDMS template mixed in 1 : 20 crosslinker : monomer ratio was not sticky and did not leave residues. Moreover, it was important for microfluidic applications because it enabled leakage-tight sealing to flat glass and PDMS substrates.

Whilst a softer PDMS can also be obtained by partially curing the PDMS in a shorter curing time, this is not recommended as it increases the variability. Inspection of incompletely cured

Table 1 *E*-Modulus of PDMS templates with different amount of crosslinking

| | Crosslinker : monomer ratios | | |
|---|---|---|---|
| | 1 : 10 (RSD, %) | 1 : 15 (RSD, %) | 1 : 20 (RSD, %) |
| *E*-Modulus, N $mm^{-2}$ | 1.1 (2.1%) | 0.6 (0.8%) | 0.1 (1.2%) |

structures by SEM (*data are not shown*) revealed a highly heterogeneous replication, randomly distributed smooth areas amongst highly structured regions.

Next, PDMS prepared in 1 : 10; 1 : 15 and 1 : 20 ratios were inspected by SEM (Fig. 3). The microscopic images showed that structures obtained under 1 : 20 ratio PDMS have been replicated in greater detail *versus* templates synthesized in 1 : 15 or 1 : 10 ratios. Sub-micron scale structures of *Aegopodium podagraia* leaf (Fig. 3d–f) showed the replication of the hair-like appendages also known as trichomes.

Because both vascularit[21–28] and surface topography[3–20] can play important role for downstream applications, it was considered to be important to not only preserve the vascularity, but also the microscopic topography of the leaf. To reveal the accuracy of the replicated templates (1 : 20 ratio), a stoma of the back side of *Tilia platyphyllos* was chosen. As shown in Fig. 4, the line structure next to the stoma can be replicated with high accuracy down to a lateral size of 500 nm. A penetration depth of 90 μm was also found for *Tilia platyphyllos* replica (Fig. 4d and h). In contrast to this, the nanostructures inside the stoma unfortunately were not replicated into the PDMS using this technique.

On the next step, AFM measurements revealed 3D structure of the replicated leaf of *Tilia platyphyllos* on PDMS. The liner structure next to the stoma was transformed into the PDMS up to a height variation of several hundreds of nanometer (see Fig. S3, ESI 1†). For the depth of a hole of a stoma that was replicated into the PDMS a height of more than 1 μm was found (see Fig. S3, ESI 1†).

Remarkably that produced PDMS replicates (1 : 20 ratio) showed also an excellent chemical stability estimated by HS-GC-MS *versus* pure PDMS matrix that maybe important in the future for bio-applications (for more information see Fig. S4, ESI 1;† HS-GC-MS chromatograms showed for pure PDMS matrix, natural *Tilia platyphyllos* leaf after contact with PDMS and PDMS template after contact with a *Tilia platyphyllos* respectively).

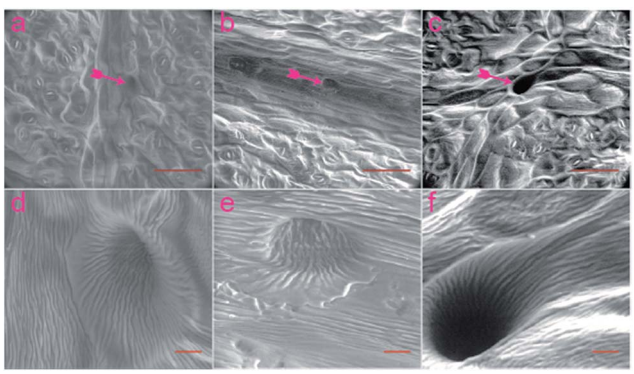


Fig. 3 SEM images of PDMS replica from *Aegopodium podagraia* leaf. (a) PDMS elastomer prepared at 1 : 10. (b) 1 : 15, and (c) at 1 : 20 initiator : monomer ratios. (d) Image of micro-hole in (a). (e) Enlarged image of micro-hole in (b). (f) Enlarged image of micro-hole in (c). Purple arrows represent the position of microholes replicated from trichomes. Scale bars (a)–(c) 100 μm, (d)–(f) 10 μm.

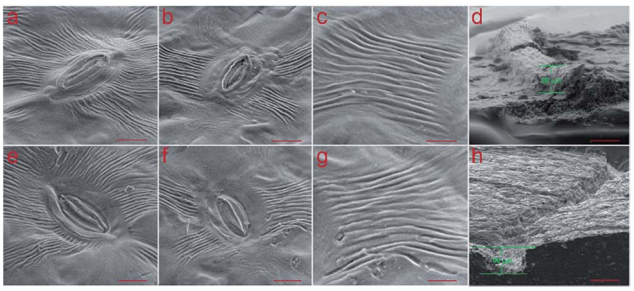


Fig. 4 SEM images of *Tilia platyphyllos* leaf and corresponding PDMS replica. (a)–(d) image of *Tilia platyphyllos* leaf. (e)–(f) PDMS replica from *Tilia platyphyllos* leaf with the same microvascular position in (a)–(d). Scale bars (a), (b), (e) and (f) 10 μm, (c) and (g) 5 μm, (d) and (h) 100 μm.

### Influence of the storage conditions of leaves templates on the soft lithography efficiency

Having optimized the casting conditions using *Aegopodium podagrai* and *Tilia platyphyllos* (see above), the fidelity of replication and structural diversity between plant species were studied using *Plantago lanceolate*, *Viburnum davidii*, and *Glechoma hederacea*. SEM images of the original leaves (Fig. 5a–c) confirmed the diversity in surface morphology between the species. The SEM images at low magnification revealed a variety of surface features. Fig. 5d–i confirmed this diversity is transferred into the PDMS replica, with biodiversity in both vascularity and surface topology preserved using plant leaves directly as template in soft lithography. The 800× images showed the stoma, the mouth-like features used for gas exchange, was also replicated well into PDMS. It is well known that cells culture in a more biologically realistic manner on structures that are not smooth but structured. Studies using the PDMS plant replicas in our laboratory have confirmed a more *in vivo*-like migration pattern for human melanoma cells (in submission – LC-TIN-01-2016-000076).

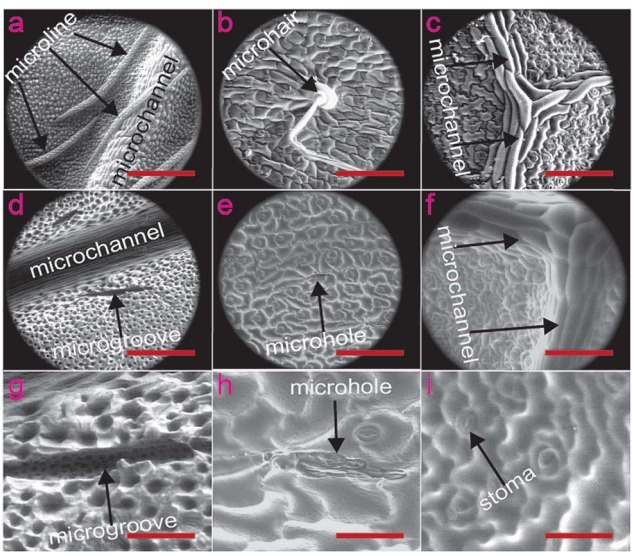


Fig. 5 SEM images of PDMS replica (1 : 20) and real leaf. (a) Leaf-template *Viburnum davidii*. (b) Leaf of *Plantago lanceolate* (c) *Glechoma hederacea* leaf. Scale bars in (a)–(f) 200 μm, (g)–(i) 50 μm.

Whist the biodiversity between leaves provides a wide variety of structures, this means the optimal leaf for a certain bioassay may have to be identified experimentally. Additionally, the precise size and geometry between leaves will vary, which may introduce an unwanted variability between studies conducted with PDMS replicates from different leaves.

To avoid this issue, and the seasonal dependence, the longevity of the templates was investigated. Initially, fresh leaves (processed on the same day they were picked) were used as templates for replication in PDMS to avoid the structural changes as the leaf dehydrates. The template was then again covered with PDMS and stored for up to a year. The *Tilia platyphyllos* template (Fig. 6a) has been replicated into PDMS for at least thirty times over a one year period. The discoloration of the leaves (Fig. 6d) indicates oxidative processes as well as the loss of water through the permeable PDMS. When comparing 'b' and 'e', some shriveling and loss of microscale features can be observed after a year storage, but a surprisingly high level of detail of the microstructures is preserved, as indicated by the SEM images of the stomata (Fig. 6f).

As aforementioned, low heated temperature of 45 °C was required for the curing of PDMS on fresh leaf template to preserve the microscopic structure. In the other case, the template would change color from green to black and microstructures were found to have collapsed. Interestingly, it was found that for aged templates stored over three months, the use of higher temperatures like 70 °C or 80°C could be used for curing PDMS without damaging the template. Whilst creating a daughter template from the first PDMS replica, for example NOA 63 resist,[35] will guarantee uniformity across the replicated structures, the ability to store the templates over an extended period of time adds to the versatility of the approach. Longevity of the *Carpinus betulus* leaf template was also investigated, indicating similar endurance results as *Tilia platyphyllos* leaf (Fig. S5, ESI 1†).

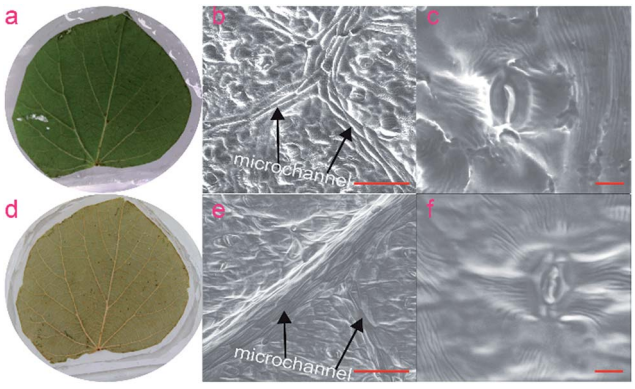


Fig. 6 *Tilia platyphyllos* leaf stored in PDMS for one year, utilized for microfabrication of over thirty times during this period. (a) Photograph of freshly prepared *Tilia platyphyllos* leaf. (b) PDMS replica from fresh *Tilia platyphyllos* leaf showing microvascular structure. (c) Imprint of stomata in PDMS replica from fresh *Tilia platyphyllos* leaf. (d) Photograph of *Tilia platyphyllos* leaf after one year. (e) PDMS replica from 1 year old *Tilia platyphyllos* leaf showing microvascular structure (f) SEM image of PDMS replica of stomata from one year old *Tilia platyphyllos* leaf. Scale bars (b) and (e) 100 μm, (c) and (f) 10 μm.

## Flow through vascular network

Water transport is one of the most important function of natural leaves. Noticeably, such complicated process totally depends on self-activated pumping with only one stiped inlet. Inspired by this post, we innovated self-powered autonomous flow inside biomimetic PDMS leaves without the need for access holes other than the inlet, to visually reveal how autonomous flow behaves inside leaves' microvasculature. Similar to real leaves, herein fluidic filling into PDMS leaves was totally self-activated, and thus, requiring very low energy[46–48] consumption.

Assuming the air in the syringe behaves as an ideal gas, Boyles law $P_1V_1 = P_2V_2$ can be used to predict the pressure[47,48] applied at the inlet of the microvascular network by compressing the air in the syringe to be approximately 2.6 atm (260 kPa). This pressure can be used to fill the microfluidic network with the ink, using the gas-permeability of PDMS to squeeze the air out. Altogether three PDMS leaves (Fig. 7) were directly replicated from natural leaves (*Tilia platyphyllos*, *Aegopodium podagraia* and *Carpinus betulus*) for flow studies, with significant differences in their microvascular networks. The flow studies were used to compare the hydrodynamic resistance of the 1st and 2nd-ordered channels branching off the main vein (Fig. S6, ESI 1†). Image analysis revealed the average flow rate in the 1st-ordered microchannels and 2nd-ordered microchannels were 0.08 mm $s^{-1}$ ($n = 1$) and 0.04 mm $s^{-1}$ (STDV, $n = 16$) for *Carpinus betulus*, 0.16 mm $s^{-1}$ (STDV, $n = 5$) and 0.11 mm $s^{-1}$ (STDV, $n = 7$) for *Aegopodium podagraia*, and 0.45 cm $s^{-1}$ (STDV, $n = 5$) and 0.22 cm $s^{-1}$ (STDV, $n = 10$) for *Tilia platyphyllos* (Fig. S7, ESI 1†). Based on flow analysis inside PDMS leaves, average flow rate through first-ordered microchannels was 1.5–2.2 times faster than flow rate in the second order channels (ESI 2, 3†), ranging from *Aegopodium podagraia*, *Carpinus betulus* and *Tilia platyphyllos* leaves. The higher flow rate in 1st microchannel than 2nd ordered microchannels, indicates geometrical microvascular configuration in leaves obtained higher overall hydraulic conductivity in first-ordered microchannels. The flow hierarchy used in plant leaves to ensure equal distribution of nutrients was preserved in the PDMS leaves with replicated fluidic structure.

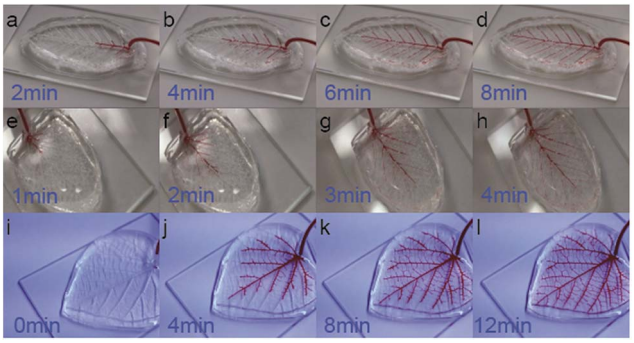


Fig. 7 Hydrodynamic filling of PDMS leaves: (a)–(d) *Carpinus betulus*, (e)–(h) *Aegopodium podagraia*, and (i)–(l) *Tilia platyphyllos*, images were obtained at 2 min, 1 min, and 4 min intervals, respectively.

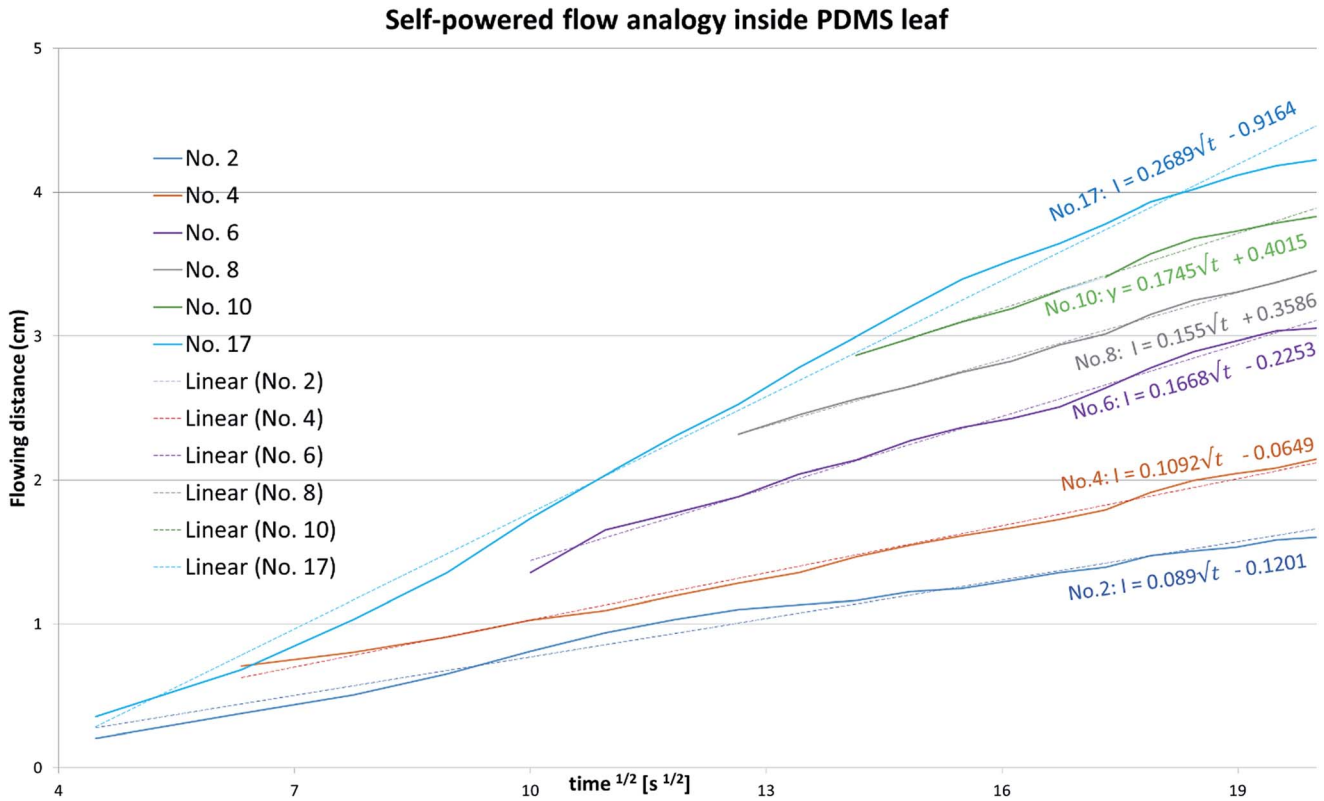


Fig. 8 Quantitative flow analogy inside PDMS leaf containing parallel networks replicated from *Carpinus betulus*, with flowing distance plotted *versus* square root of time.

Total filling time of all three PDMS leaves was less than 10 minutes, indicating suitability for loading medium for static cell culture. Accounting that both plant leaves and animal circulatory systems are nature evolved microfluidic channels[51] obeying Murray's law,[27] plant leaves may become attractive templates to fabricate biomimetic microvascular devices for further animal cell studies.

Further analysis of the flow rate in both the 1st microchannel (no. 17) and 2nd ordered microchannels (no. 2, 4, 6, 8, 10) of PDMS leaf from *Carpinus betulus* (Fig. S8, ESI 1†), also surprisingly showed that the flow in leaf-inspired microvascular channel obeys sorptivity rule,[49,50] which is mostly found in capillary absorption, and can be represented by the following equation,

$$I = S\sqrt{t}$$

where $I$ is the cumulative flow amount, $S$ is sorptivity constant, and $t$ is time.

It's seen from Fig. 8, the flowing distance (amount) in both the 1st microchannel and the 2nd ordered microchannels of PDMS leaf from *Carpinus betulus*, were linearly correlate with the square root of time, obeying sorptivity rule.

## Conclusion

A simple method for the replication the venation pattern and microscopic surface morphology – down to a lateral size of 500 nm of plant leaves into PDMS is presented by directly using the leaves as template. The method was applied to leaves from over ten different species, covering the most common reticulate, arcuate, pinnate, parallel and palmate venation patterns. The soft lithography process was optimised by reducing the initiator to monomer ratio from 1 : 10 to 1 : 20 to make a softer PDMS, which allows for a leakage-tight seal with a flat substrate despite the surface topography. Using reversibly bound PDMS on glass devices, no leakages were observed when filling the microfluidic network with pressures up to 260 kPa. Evaluation of the linear flow velocities in 1st and 2nd order microchannels revealed the linear flow rate in the 2nd order channels was about half of that in the 1st order structure, facilitating ordered filling of the leaf. It's surprisingly found here that flow in both 1st and 2nd ordered microchannels of PDMS leaf from *Carpinus betulus*, obeys sorptivity rule that's believed mainly applied to capillary absorption in conventional views. We'll make a deeper study on this discovery in our future work.

With a demonstrated ability to replicate from a wide variety of vascular structures, this methodology provides access to a variety of fluidic structures, with an even larger variety in functionality provided by presence, location and structure of micro- and nanometer scaled structures caused by structures like stomata and trichomes. The surface of leaf-replicated channels is not smooth and may be more bioequivalent than lithographically fabricated structures, with preliminary studies confirming a more *in vivo*-like migration pattern for human

 

melanoma cells. The variety in three dimensional vascularity and inhomogeneous surfaces offered by this new, simple and affordable approach for biomimetic microfabrication may benefit many *in vitro* cell-based assays.

## Acknowledgements

The authors would like to thank Karsten Brill (KIST) for SEM images, Florian Warnke (KIST) for assistance in identifying leaves species, JuYeol Bae (Pusan National University, Korea) for assistance in preparing samples, Sarah Fischer (INM) for Elastic-modulus measurements and Franziska Emmerich (INM) for excellent AFM images. RMG would like to acknowledge the Alexander von Humboldt Foundation for a fellowship.

## Notes and references

1 S. Mann, *Biomineralization, Principles and Concepts in Bioinorganic Materials Chemistry*, Oxford University Press, Oxford, 2001.
2 M. Liu, Y. Zheng, J. Zhai and L. Jiang, *Acc. Chem. Res.*, 2010, **43**, 368.
3 E. Mele, S. Girardo and D. Pisignano, *Langmuir*, 2012, **28**, 5312.
4 Z. Yuan, H. Chen, J. Tang, H. Gong and Y. Liu, *J. Phys. D: Appl. Phys.*, 2007, **40**, 3485.
5 C. Liu, *Microfluid. Nanofluid.*, 2010, **9**, 923.
6 W. Zhao, L. Wang and Q. Xue, *J. Phys. Chem. C*, 2010, **114**, 11509.
7 M. Sun, C. Luo, L. Xu, H. Ji, Q. Ouyang, D. Yu and Y. Chen, *Langmuir*, 2005, **21**, 8978.
8 M. Liu, Y. Zheng, J. Zhai and L. Jiang, *Acc. Chem. Res.*, 2010, **43**, 368.
9 B. Deng, R. Cai, Y. Yu, H. Jiang, C. Wang, J. Li and L. Li, *Adv. Mater.*, 2010, **22**, 5473.
10 J. Wang, Y. Zheng, F. Q. Nie, J. Zhai and L. Jiang, *Langmuir*, 2009, **25**, 14129.
11 W. Choi, A. Tuteja, S. Chhatre and J. M. Mabry, *Adv. Mater.*, 2009, **21**, 2190.
12 M. J. Hancock, K. Sekeroglu and M. C. Demirel, *Adv. Funct. Mater.*, 2012, **22**, 2223.
13 X. F. Gao, X. Yan, X. Yao, L. Xu, K. Zhang and J. H. Zhang, *Adv. Mater.*, 2007, **19**, 2213.
14 Z. Zhang, T. Zhang, Y. W. Zhang, K. S. Kim and H. Gao, *Langmuir*, 2012, **28**, 2753.
15 M. Xiao, M. Cheng, Y. Zhang and F. Shi, *Small*, 2013, **9**, 2509.
16 Y. C. Jung and B. Bhushan, *J. Phys.: Condens. Matter*, 2010, **22**, 035104.
17 G. D. Bixler and B. Bhushan, *Nanoscale*, 2013, **5**, 7685.
18 A. Solga, Z. Cerman, B. F. Striffler, M. Spaeth and W. Barthlott, *Bioinspiration Biomimetics*, 2007, **2**, S126.
19 T. S. Wong, S. H. Kang, S. K. Y. Tang, E. J. Smythe and B. D. Hatton, *Nature*, 2011, **477**, 443.
20 X. Wang, X. Liu, F. Zhou and W. Liu, *Chem. Commun.*, 2011, **47**, 2324.
21 M. Kobayashi, *Comm. Nonlinear Sci. Numer. Simulat.*, 2010, **15**, 787.
22 D. L. Royer, P. Wilf, D. A. Janesko, E. A. Kowalski and D. L. Dilcher, *Am. J. Bot.*, 2005, **92**, 1141–1151.
23 H. F. Huang, Q. X. Chu and J. K. Xiao, *IEEE Trans. Electromagn. Compat.*, 2010, **52**, 759.
24 M. Coppens, *Ind. Eng. Chem. Res.*, 2005, **44**, 5011.
25 W. Liu and Y. Zhang, *Adv. Nat. Sci.*, 2010, **3**, 82.
26 R. F. Service, *Science*, 2011, **334**, 925.
27 C. A. Price, S. J. C. Knox and T. J. Brodribb, *PLoS One*, 2013, **8**, e85420.
28 K. A. McCulloh, J. S. Sperry and F. R. Adler, *Nature*, 2003, **421**, 939.
29 C. S. Effenhauser, G. Bruin, A. Paulus and M. Ehrat, *Anal. Chem.*, 1997, **69**, 3451.
30 W. Wu, J. Wu, J. H. Kima and N. Y. Lee, *Lab Chip*, 2015, **15**, 2819–2825.
31 W. Wu, K. T. Kang and N. Y. Lee, *Analyst*, 2011, **136**, 2287.
32 W. Wu, K. T. L. Trinh and N. Y. Lee, *Analyst*, 2012, **137**, 2069.
33 W. Wu, K. T. L. Trinh and N. Y. Lee, *Analyst*, 2012, **137**, 983.
34 W. Wu and A. Manz, *RSC Adv.*, 2015, **5**, 70737.
35 W. Wu and N. Y. Lee, *Anal. Bioanal. Chem.*, 2011, **400**, 2053.
36 W. Wu, C. J. Hansen, A. M. Aragón, P. H. Geubelle, S. R. White and A. Lewis, *Soft Mater.*, 2010, **6**, 739.
37 W. Wu and N. Y. Lee, *Sens. Actuators, B*, 2013, **181**, 756.
38 H. J. Koo and O. D. Velev, *Sci Rep.*, 2013, **3**, 2357.
39 X. Noblin, L. Mahadevan, I. A. Coomaraswamy and D. A. Weitz, *Proc. Natl. Acad. Sci. U. S. A.*, 2008, **105**, 9140.
40 J. He, M. Mao, Y. Liu, J. Shao, Z. Jin and D. Li, *Adv. Healthcare Mater.*, 2013, **2**, 1108.
41 I. Wagner, E. Materne, S. Brincker, U. Süßbier, C. Frädrich, M. Busek, F. Sonntag, D. A. Sakharov, E. V. Trushkin, A. G. Tonevitsky, R. Laustera and U. Marxa, *Lab Chip*, 2013, **13**, 4697.
42 I. Maschmeyer, A. K. Lorenz, K. Schimek, T. Hasenberg, A. P. Ramme, J. Hübner, M. Lindner, C. Drewell, S. Bauer, A. Thomas, N. Sambo, F. Sonntag, R. Lauster and U. Marx, *Lab Chip*, 2015, **15**, 2688.
43 K. Schimek, M. Busek, S. Brincker, B. Groth, S. Hoffmann, R. Lauster, G. Lindner, A. Lorenz, U. Menzel, F. Sonntag, H. Walles, U. Marxa and R. Horland, *Lab Chip*, 2013, **13**, 3588.
44 X. Liu, M. Mwangi, X. Li, M. O'Brien and G. Whitesides, *Lab Chip*, 2011, **11**, 2189.
45 K. A. Shaikh, K. Ryu, E. Goluch, J. Nam, J. Liu, C. Thaxton, T. N. Chiesl, A. E. Barron, Y. Lu, C. Mirkin and C. Liu, *Proc. Natl. Acad. Sci. U. S. A.*, 2005, **102**, 9745.
46 I. K. Dimov, L. Basabe-Desmonts, J. L. Garcia-Cordero, B. M. Ross, A. J. Ricco and L. P. Lee, *Lab Chip*, 2011, **11**, 845.
47 W. Wu, K. T. L. Trinh and N. Y. Lee, *RSC Adv.*, 2015, **5**, 12071.
48 W. Wu, K. T. L. Trinh and N. Y. Lee, *Analyst*, 2015, **140**, 1416.
49 C. Hall and W. D. Hoff, *Water Transport in Brick, Stone and Concrete*, CRC Press, 2012.
50 R. Siddique, *Construct. Build. Mater.*, 2013, **47**, 1444.
51 L. Hu, H. Zhou, H. Zhu, T. Fan and D. Zhang, *Soft Matter*, 2014, **10**, 8442.